

A Simple, Accurate Texture Model for Woven Cotton Cloth

Piti Irawan*

Stephen R. Marschner†

Cornell University Program of Computer Graphics

Abstract

Cotton cloth is a commonly encountered material in everyday life, and a realistic model for its appearance is needed for rendering clothing and environments in many computer graphics applications. For realism it is important to produce the correct texture when the pattern of threads is resolved in the image, but cloth must also be rendered efficiently in more distant views when the thread pattern is not resolved. This paper introduces a simple model that, for any view and illumination directions, reproduces both the small-scale texture (BTF) and the large-scale reflectance (BRDF) of woven cloth within a single framework. The model is simple and fast, and it can handle any weave pattern using only a small set of parameters. The model is validated against measurements, and it qualitatively matches both the texture and reflectance observed in real cloth.

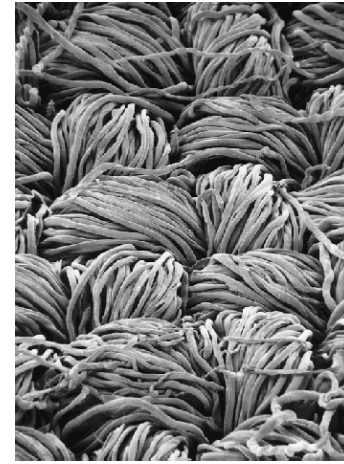


Figure 1: A typical plain weave fabric. Image from [USDA 2005a].

1 Introduction

Cloth is an important material to render convincingly because it appears regularly in computer graphics scenes, especially those involving virtual humans in everyday environments. Fabric appearance is also important in industrial applications of computer graphics in the textile, garment, and fabric care industries. Our goal is to develop a simple, easy-to-use model of cloth that efficiently captures the important features of its appearance.

Cotton constitutes over 40 percent of the world’s fiber production, more than any other textile fiber [USDA 2005b], and for this reason modeling cotton is a logical first step toward a model for the appearance of fabric in general.

In scenes rendered for computer graphics, the aspects of cloth appearance that are important to capture in a model for rendering include:

- The texture of the weave pattern, which is needed to render more close-up views in which the weave pattern is resolved in the image. Each weave has its own distinctive texture, which is an important part of its appearance.
- The directional reflectance (BRDF), which describes the overall distribution of light reflected from a large (more than 1–2 mm across) area of fabric.

We assume that a general-purpose cloth model needs to be realistic at image resolutions up to 2 or 3 pixels per thread, when threads are resolved but not individual fibers. Resolutions higher than this are in the realm of macrophotography and would need to be rendered using a complete model of the cloth’s three-dimensional structure.

A detailed cloth model that includes the weave texture can, of course, be rendered from any viewing distance. However, if only the texture is available, distant views in which the weave pattern is not resolved become very difficult antialiasing problems, causing artifacts and poor performance. For this reason a BRDF model that

matches the texture is mandatory in any practical model for cloth appearance.

To be most useful in practice, a model should also make efficient use of memory and processing time, and it should be controlled by a small number of parameters whose function is easy to understand.

In this paper we introduce a new model for the appearance of woven cotton cloth, which was motivated by, and is validated against, detailed BTF measurements of real fabric. The model is simple and efficient, works for arbitrary weave patterns, does not rely on stored appearance data, and is controlled by a few simple parameters. It defines a BTF and BRDF that are analytically equivalent at large scales, and it is shown to qualitatively match the measured appearance of real cloth.

1.1 Prior Work

While most of the work on modeling cloth for computer graphics has focused on motion rather than appearance, several researchers have addressed the problem of rendering cloth.

Cloth often appears as an example of a material with an unusual BRDF. Westin et al. [1992] computed BRDFs for velvet and plain-weave nylon fabrics by ray tracing models of the small-scale struc-

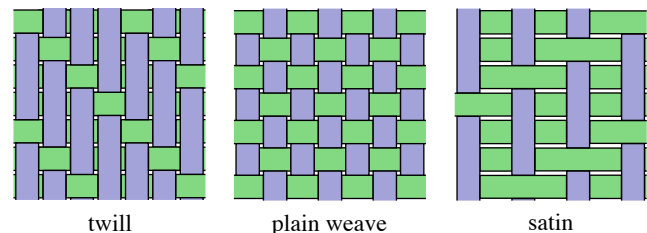


Figure 2: Examples of the three common weave patterns.

*e-mail:irawan@cs.cornell.edu

†e-mail:srm@cs.cornell.edu

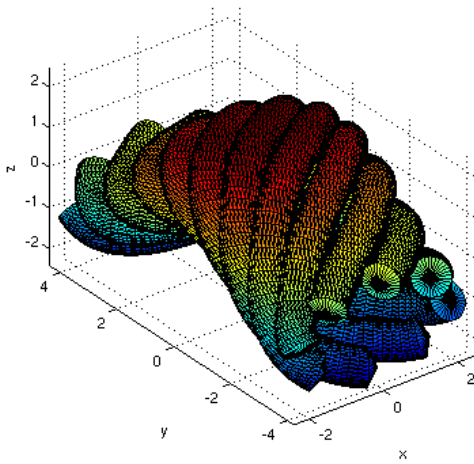


Figure 3: 3D model of a thread.

ture. Similarly, Volevich et al. [1997] used curved infinite cylinders to model a piece of artificial silk and ray traced it to obtain its bidirectional scattering distribution function. Velvet [Lu et al. 1998], satin [Ngan et al. 2005], and patterned upholstery [McAllister et al. 2002] have been subjects of BRDF measurement studies for computer graphics and vision. Ashikhmin et al. [2000] used a linear combination of two cylindrical Gaussian slope distributions to model satin in their microfacet-based BRDF generator. All this work assumes the weave texture is not visible, and the models and measurements have not been validated against one another.

Other works have focused on the structure and texture of fabric. Adabala et al. [2003] presented a method based on a microfacet model and procedural textures that is capable of rendering clothes with a variety of weave patterns at different levels of detail. Unfortunately, no data were presented to support the appearance of the clothes and the lack of examples of the model on simple weave patterns makes it hard to judge its correctness. Xu et al. [2001] used a volume rendering approach for close-up views of coarse knit fabrics. Taking a data-based approach, Sattler et al. [2003] measured, stored, and retrieved bidirectional texture function (BTF) data as needed to render clothes. The cloth looks good and the appearance is supported by data. However, large storage space is required and it is only possible to model the specific fabrics that have been captured. Drago and Chiba [2004] modeled woven canvases (commonly used for painting) by Nurbs surfaces that are shaded by a procedural texture.

The rest of this paper is structured as follows. In Section 2, we explain the characteristics cotton cloth and the expected behavior of the specular highlight texture based on a simple 3D model of the fabric’s mesostructure. The details of our measurements are described in Section 3. Section 4 and 5 contain the main contributions of this paper: a BTF model that can be used both for close-up and far-away views of the cloth and a BRDF model that exactly matches the BTF and allows for faster far-away views of the cloth. We present some results in Section 6 and conclude in Section 7.

2 Structure and reflection in cloth

Cotton fibers consist of cellulose and, when dried, have flat and twisted ribbon-like shapes. Cotton threads are made by twisting the fibers around each other, with the friction between the fibers alone serving to hold them together.[Welford 1967] Because of this twisted structure, the fibers on the surface of a woven fabric appear

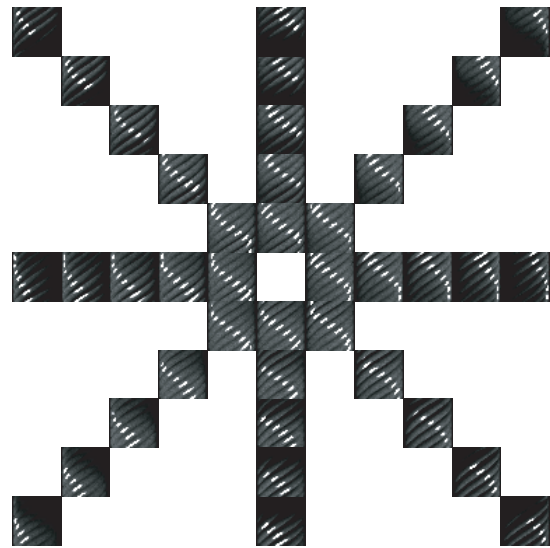


Figure 4: Ray-traced images of the model in Figure 3. Camera is directly above the model. Position in the grid indicates the direction of the light source.

in a diagonal arrangement, with alternating directions for exposed parts of the warp and weft threads, as can be seen in Figure 1.

Woven cloth is constructed by interlacing two sets of parallel threads, known as the *warp* and *weft* (in this paper we observe the convention that the warp threads run vertically in the figures). The pattern in which the warp and weft are interleaved varies greatly, but the majority of cotton fabrics are made in one of the three simplest weave patterns: plain weave (roughly 80%), twill, and satin [Parker 1993] (Figure 2). Therefore, it is reasonable to start with cotton clothes in those weave patterns. In this paper, we use twill cloth in the majority of the examples because of the clarity of its threads and the highly visible texture the threads make.

By analyzing how light is expected to reflect from the geometric structure of cotton cloth, we can understand what key behaviors to expect in the measurements and how they can be qualitatively reproduced in a practical model.

Individual fibers are quite smooth and may be expected to reflect light specularly; light that enters the mass of fibers below the surface will contribute to diffuse reflection, and in the black cloth we measured will mainly be absorbed. Individual random variations in fiber orientation will serve to blur the specular highlight (for small variations) or to contribute to diffuse reflection (for “flyaway” fibers). To get a qualitative idea of highlight motion, therefore, an idealized helical structure can be used.

Based on these observations we built a simple model (Figure 3) of cylinders spiraling around a thread, with the whole thread bent into a shape consistent with woven cloth. Rendering a small section of a few such threads interlocked in a plain weave gives an idea of what changes in appearance are consistent with specular reflection from the cotton fibers. The surfaces of the cylinders are treated as specular, with a small diffuse component to make the images more understandable. Views of a single thread section for varying light source direction are shown in Figure 4.

The main characteristic of these images is a diagonal highlight that maintains roughly the same orientation as it moves around in the image. This feature is also seen in the measurements, and it is based on these moving diagonal highlights that the BTF model is based.

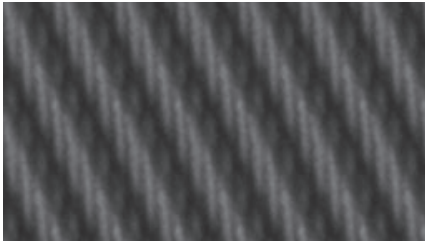


Figure 5: Close up view of a twill cloth.

Rendering an entire sheet of fabric using this 3D model would be prohibitively slow, and is unnecessarily detailed for normal viewing distances. We shall describe a simple and fast way to produce the highlight by exploiting its regularity in Section 4.

3 Measurements

Our BTF and BRDF model is designed to match both the large-scale BRDF and the medium-scale texture of cloth samples measured in the laboratory. After examining several types of cloth we concluded that the most instructive type to focus on was woven cotton cloth that is dyed black. Woven cloth in common weave patterns was chosen because it is commonly used in clothing and therefore a useful example to study, and black was chosen to isolate the texture caused by specular reflection from the fibers.

The measurements consisted of illuminating a sample of cloth with a small light source and photographing it through a macro lens at a magnification that enabled the threads to be clearly discerned. Sets of images were taken with the source fixed and camera moving to many points over the hemisphere, and with the camera fixed and the source moving to many points over the hemisphere. All measurements were made with fiducial markers resting on the cloth surface¹; these markers were located in the images and used to align the frames and resample them into a common coordinate system aligned with the surface of the cloth.

In the raw measurement images, the overall pattern is difficult to discern because of the natural irregularities of the threads. To remove this random variation and make the systematic pattern more visible, we computed a perfectly regular tiled pattern by averaging all the unit tiles in the measured image, then tiling the image with the resulting average tile. A representative frame from the measurements is shown in Figure 5, and more measurements can be seen in the accompanying video.

Looking at the measurement data, a behavior qualitatively similar to the rendered 3D model is observed: the highlights are elongated and tilted, and they appear to slide around in the image without changing shape appreciably. (The highlight motion in the data is best appreciated from the accompanying video.)

The data show the change in the highlight texture with illumination direction. In another set of data, we observed the same change in texture with viewing direction. The data are compiled and grouped by their half vector — which bisects the angle between the incident and exitant directions — in Figure 6. Images in a column have a similar texture appearance and we can conclude that texture is a

¹For image sets including oblique camera angles, it was necessary to estimate and compensate for the distance above the cloth at which the markers rested.



Figure 6: Measurement images grouped in columns based on their half vector. Two pairs of numbers under the images are the incident and exitant directions. Note the similarity of the images in a column.

function of the half vector. BRDF measurements of cloth (attenuated by the cosine of the incidence angle) can be obtained by taking the average value of each image. Designing a BTF to reproduce the texture and match the BRDF is the topic of the following section.

4 BTF Model

In this section, let the origin be the lower left corner of the rectangular window for a particular thread segment with the x axis pointing to the right, along the length of weft threads, and the y axis pointing upward, along the length of warp threads. Surface normal \mathbf{n} is the vector $(0, 0, 1)$.

Dana et al. [1999] introduced Bidirectional Texture Functions (BTFs) to describe the appearance of texture as a function of incoming and outgoing directions. It is, hence, a 6D function

$$L(\mathbf{p}, \mathbf{v}_i, \mathbf{v}_o) \tag{1}$$

that returns the reflectance at point \mathbf{p} illuminated from \mathbf{v}_i and seen from \mathbf{v}_o . In this paper we express the BTF in the same units as the BRDF, meaning that the reflected radiance is the product of the BTF with the irradiance on the plane where the BTF is defined. This means the BTF values do not drop off with $\mathbf{n} \cdot \mathbf{v}_i$ because that factor is built into the irradiance. Under this definition, averaging the BTF values for all points \mathbf{p} on a surface illuminated from \mathbf{v}_i and seen from \mathbf{v}_o yields the BRDF value of the surface illuminated and seen from the same directions. We will use this fact in Section 5.

A piece of cloth is made of warp and weft threads according to a weave pattern. Disregarding random variations, the visible segments of the warp threads all have the same appearance, as do the visible segments of the weft threads. Therefore, once we define the BTFs of the segments, we can construct the cloth by tiling identical segments according to the weave pattern.

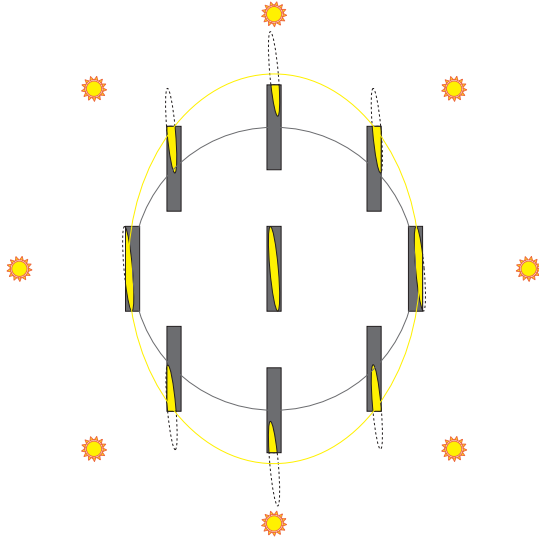


Figure 7: Illustration of our BTF model on a warp segment of a twill cloth. The ellipse moves according to the illumination direction and gets clipped by the rectangular window.

From examining the measurement data, we can describe the key behaviors of the specular highlight as follows:

1. The shape of the highlight is roughly an angled ellipse.
2. The part of this ellipse that falls outside the segment is invisible.
3. The center of this ellipse moves according to the half vector between the incident and exitant directions.

Our new BTF model simply encodes these observations in an empirical model for the highlight, while including the appropriate factors so that when the BRDF is computed it will have the standard microfacet form. The texture for a given viewing/illumination configuration is made up of two colors, a specular color that appears inside the highlight and a diffuse color that appears outside the highlight. Let \mathbf{h} be the half vector and θ_d be half the angle between \mathbf{v}_i and \mathbf{v}_o . The specular intensity changes with viewing configuration:

$$L(\mathbf{p}, \mathbf{v}_i, \mathbf{v}_o) = k_d + k_s \frac{I(\mathbf{p}, \mathbf{h})F(\theta_d)G(\mathbf{v}_i, \mathbf{v}_o)}{\mathbf{v}_i \cdot \mathbf{n} \mathbf{v}_o \cdot \mathbf{n}}$$

The diffuse and specular coefficients k_d and k_s control the color and brightness of specular and diffuse reflection; the highlight texture function $I(\mathbf{p}, \mathbf{h})$ returns 1 or 0 depending on whether the point \mathbf{p} lies in a highlight or not; $F(\theta_d)$ is the Fresnel function evaluated at θ_d ; and $G(\mathbf{v}_i, \mathbf{v}_o)$ is the Torrance-Sparrow shadowing/masking function. This equation is exactly a microfacet BRDF, but with the function I taking the place of the slope distribution.

To understand the basic operation of our highlight model $I(\mathbf{p}, \mathbf{h})$ in a single thread segment, think of the segment as a rectangular window through which an angled ellipse is seen (Figure 7). To evaluate I we compute the ellipse's location based on the half vector, then return 1 if the shading point is inside that ellipse or 0 otherwise. Note that all the computations are done without any reference to the actual geometry of the weave; the BTF is defined directly on a plane. Occlusion and shadowing are not handled explicitly; rather they are empirically modeled by allowing the highlight to slide out of the window and by scaling its intensity using the shadowing/masking function. We shall illustrate the process by modeling a warp segment to match Figure 5.



Figure 8: Our BTF model on twill cloth.

For this fabric the warp segment is long and thin, with a width:height ratio of about 1:6, so we set the segment size to $(s_x, s_y) = (1.0, 6.0)$.

We compute the center of the ellipse (c_x, c_y) as follows.

$$\begin{pmatrix} c_x \\ c_y \end{pmatrix} = \begin{pmatrix} \frac{1}{2}s_x(k_x h_x + 1) \\ \frac{1}{2}s_y(k_y h_y + 1) \end{pmatrix} \quad (2)$$

The vector (h_x, h_y) is the projection of the half vector onto BTF plane, and it determines the offset of the highlight. The constants k_x and k_y scale the offset to control how far the highlight moves from the center of the rectangular window.

The elliptical highlight can be described by its semimajor axis α and its eccentricity η . The highlight is thin and elongated in the same general direction as the segment, so we choose $(\alpha, \eta) = (3.0, 0.995)$. It is also rotated slightly counterclockwise of vertical, so we let $\phi_E = 95^\circ$.

The two foci of the ellipse, \mathbf{F}_1 and \mathbf{F}_2 , are offset from the point (c_x, c_y) along the ellipse's major axis by a distance η :

$$\mathbf{F}_{1,2} = \begin{pmatrix} c_x \\ c_y \end{pmatrix} + R(\phi_E) \begin{pmatrix} \pm\alpha\eta \\ 0 \end{pmatrix} \quad (3)$$

To check whether the point (x, y) lies inside the ellipse, recall that an ellipse is the set of points for which the sum of the distance from the two foci is exactly 2α . Therefore the value of I is simply:

$$d = \|\mathbf{F}_1 - \mathbf{p}\| + \|\mathbf{F}_2 - \mathbf{p}\| \quad (4)$$

$$I(\mathbf{p}, \mathbf{h}) = \begin{cases} 1 & \text{if } d \leq 2\alpha \\ 0 & \text{if } d > 2\alpha \end{cases} \quad (5)$$

The BTF for weft segments is defined in the same way. By tiling the warp and weft segments together, we will get the twill cotton cloth shown in Figure 8. This simple process of making individual segments and then tiling them can be done to make cotton clothes of any weave patterns.

Due to the simplicity of the model, the cost of rendering a cotton cloth with accurate close-up appearance is low. In fact, the model is readily amenable to being implemented in a GPU pixel shader. Furthermore, as we will show in Section 6, the cloth texture seen in close-up view gracefully converges to the correct BRDF for far-away view. That is, no additional strategy is required to make this fine-scale texture model match the large-scale behavior of real fabric. What is more, the BRDF can readily be computed exactly, as we show in the next section.

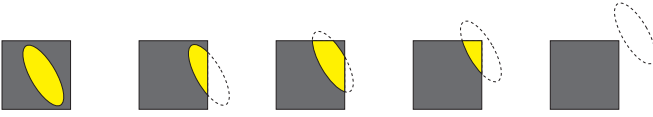


Figure 9: Five possible ellipse-rectangle combinations. From left to right: case 1 to 5.

5 BRDF Model

From a distance away, cloth texture ceases to be an important feature and BRDF is sufficient to get the correct appearance. We have said in Section 4 that the average BTF value of a surface is exactly the BRDF value of the surface. Therefore, instead of shooting many rays and computing whether they hit inside or outside the ellipse, we can compute the average reflectance value inside each of the rectangular thread segments in the weave pattern and average them, weighted by the areas of the segments, to arrive at the BRDF value.

In Equation 4 the only term that depends on position is $I(\mathbf{p}, \mathbf{h})$; the rest of the model depends solely on the directional parameters. Therefore, computing the average value of the BTF amounts to computing the average value of I . The average value of I is simply the area of the intersection of the ellipse with its window, divided by the area of the window. Once this area fraction $\bar{I}(\mathbf{h})$ is known, the average of the BTF is a microfacet BRDF, with \bar{I} as the facet normal distribution.

To do so, we need to be able to compute the area of the ellipse that falls inside the window. The steps to do this are described next.

Let \mathbf{a} and \mathbf{b} be vectors that are the semimajor and semiminor axes of the ellipse and let \mathbf{c} be the center of the ellipse. Then the homogeneous 2D transformation matrix

$$M = \begin{pmatrix} a_x & b_x & c_x \\ a_y & b_y & c_y \\ 0 & 0 & 1 \end{pmatrix} \quad (6)$$

maps the unit circle to the highlight. Applying M^{-1} to the highlight, therefore, maps it to the unit circle. The idea is to apply M^{-1} to both the ellipse and the rectangular window and compute the area of the circle that lies inside the transformed window. Let A_E be the area of the ellipse that falls inside the rectangular window and A_C the area of the circle that falls inside the transformed window; they are related by the following equation.

$$A_E = |\det M| A_C \quad (7)$$

We make an assumption that the ellipse fits inside the rectangular window—when the center of the ellipse is nailed to the center of the rectangular window, no part of the ellipse gets clipped by the window. From our experience, this assumption does not reduce how well the BTF model can match the data and, while it is not a necessity, it simplifies the BRDF model by allowing only the five cases shown in Figure 9.

We begin by computing the intersections of the circle with the perimeter of the rectangle, keeping the points in clockwise order around the rectangle. We subtract the arc tangents of pairs of intersection points to obtain the directed angles from the first to the second point of each segment of perimeter that is inside the circle.

In case 1 the ellipse is entirely inside the rectangular window and $A_C = \pi$.

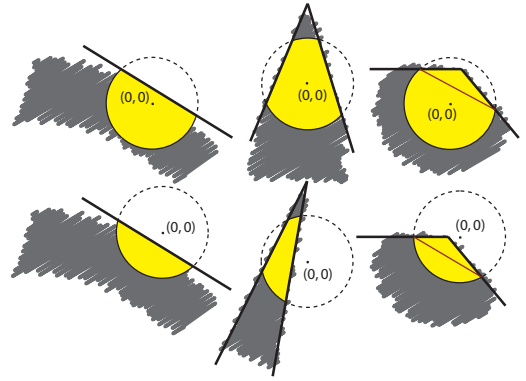


Figure 10: Details of case 2 (left column), 3 (middle column), and 4 (right column).

For cases 2–4 we need the area of a circular segment. The area of a segment of the unit circle spanned by central angle $0 \leq \theta \leq 2\pi$ is:

$$A_S(\theta) = \frac{1}{2}(\theta - \sin(\theta)) \quad (8)$$

Note that this formula works for angles up to 2π ; when $\theta > \pi$ the segment contains the origin.

In case 2 there are two intersections with the same edge. The area of the circle that lies inside the transformed window is a single circular segment and can be computed directly from (8).

In case 3 there are four intersections. The area is most conveniently computed by subtracting the two segments outside the rectangle from the area of the whole circle:

$$A_C = \pi - A_S(2\pi - \theta_1) - A_S(2\pi - \theta_2) \quad (9)$$

In case 4, there are two intersections and one corner of the transformed window is inside the circle. The resulting area can be broken into a segment and a triangle, as shown in Figure 10.

In the fifth case, the ellipse is entirely outside the rectangular window and $A_C = 0$.

Finally, let A_R be the area of the rectangular window and the area ratio is

$$S = \frac{A_E}{A_R} \quad (10)$$

6 Results

The image in Figure 11 shows the close up texture comparison with the measurement image in Figure 5 and the BTF illustration in Fig-

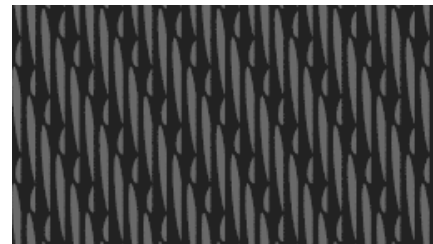


Figure 11: Close up rendering of a twill cloth

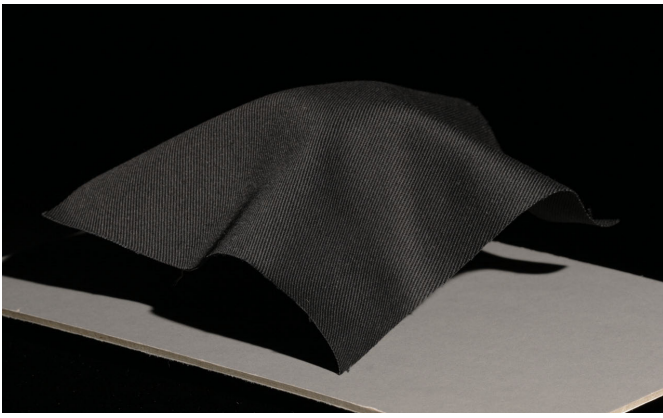


Figure 12: A 12 cm x 12 cm twill cloth.

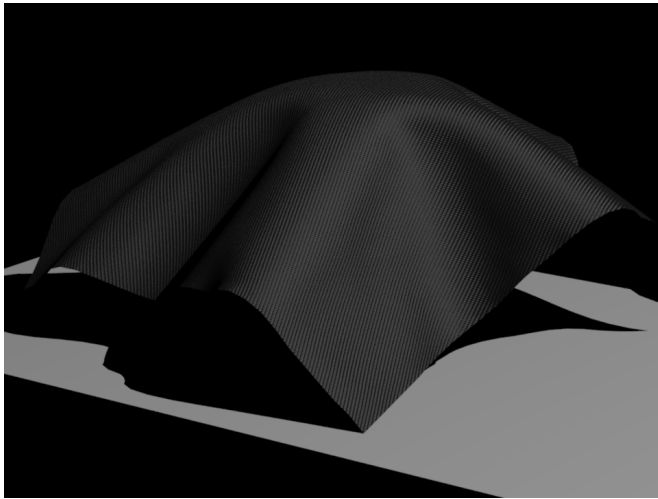


Figure 13: Rendering of a 12 cm x 12 cm twill cloth.

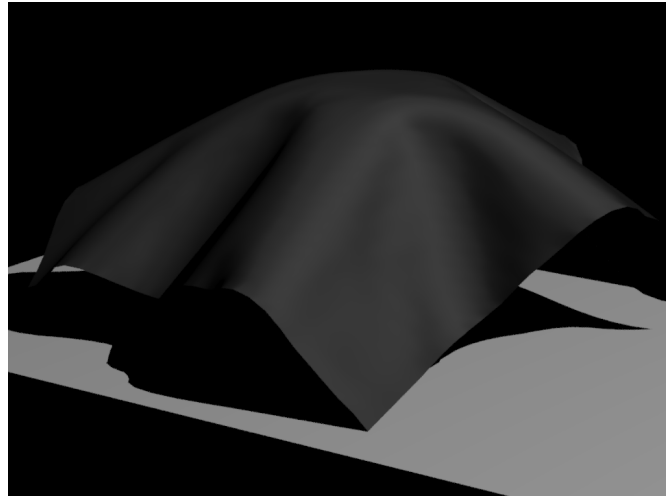


Figure 14: Rendering of a 12 cm x 12 cm twill cloth using BRDF method.

Figure 8.

However, the appearance of a cloth is considerably affected by its shape. To obtain geometry to demonstrate our models, we draped a 12 cm x 12 cm piece of twill cloth on a small metal cylinder (Figure 12) and scanned it with a laser range scanner. We then fit a cloth animation model to the scanned points to get a triangle mesh that approximates the cloth surface. We rendered this mesh with our BTf model (Figure 13) and our BRDF model (Figure 14). Both renderings were done with the following parameters for warp threads: $s_x = 1$, $s_y = 6$, $\alpha = 3$, $\eta = 0.995$, $\theta_E = 95^\circ$, $k_x = 1.5$, $k_y = 3.1$

and the following parameters for weft threads: $s_x = 1$, $s_y = 2$, $\alpha = 1$, $\eta = 0.9$, $\theta_E = 80^\circ$, $k_x = 3.7$, $k_y = 1.6$.

While differences in geometry, and the lack of random variations in the modeled fabric, prevent an exact match, the characteristic shapes of the highlights on this type of cloth are reproduced well. Also note how the texture changes from one part of the highlight to another are reproduced by the texture model. The BRDF-based rendering exactly matches the average value of the BTf-based rendering, by construction.

Comparison between the BRDF of the measurement data and the BRDF of rendered images is shown in Figure 15. In the plot, x-

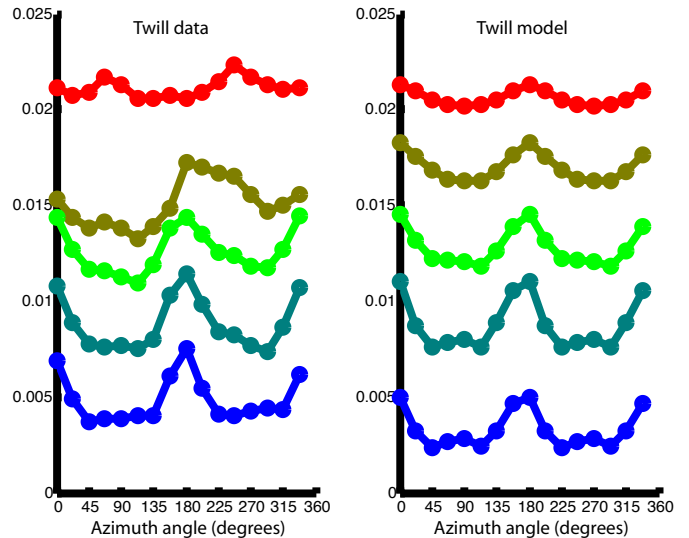


Figure 15: Twill BRDF comparison.

axis is the azimuth of the incident direction and y-axis is the BRDF value multiplied by $\mathbf{v}_i \cdot \mathbf{n}$ and scaled to match the average value of the whole dataset. The curves group the points according to the elevation angle of the incident direction; from top to bottom: 15° , 30° , 45° , 60° , and 75° . An empirical model such as ours is not expected to match the BRDF data exactly, but the trend of periodic variation in BRDF with azimuth, increasing in amplitude toward grazing elevation, is matched well by our model.

Similarly, we used our method to simulate plain weave and sateen cloth, based on measured BTF data taken in the same way as for the twill cloth. The results are seen in Figures 16 and 18. Note how both the weave texture and the highlight pattern change to reproduce the appearances of these different types of fabric.

7 Conclusion

We have proposed a very simple and efficient model for the texture of woven cotton cloth. It is an empirical model, but based on measurements of real cloth samples, and it matches the data both by visual appearance of the texture and by qualitative comparison of the BRDF. The model is simple enough to evaluate that it can be used in performance-driven applications; in fact, it should be easy to implement it to run in graphics hardware. Another great advantage due to the model's simplicity is that it can be analytically integrated to get the exact corresponding BRDF, which is also simple to evaluate, so that the transition from close to far viewing can be seamless.

This same model should apply readily to other woven fabrics with a similar thread structure: for instance, synthetic fabrics or linen. Some other fabrics' structure is quite different, however—silk fibers, for example, lie much flatter and straighter, without the twist characteristic of cotton threads. Also, knit fabrics have entirely different thread geometry, but they may be amenable to a similar approach using a more complex tile structure.

In order to isolate the specular highlight, which is the cause of the most important directional effects in this type of fabric, we have included only measurements of black material. Our preliminary investigations suggest that the diffuse component of reflection in light colored fabric contributes much less to the texture, probably because of the blurring effect of multiple scattering among the fibers. However, our texture model may need to be extended to handle medium to dark colors accurately. For thin or light colored fabrics, a model for transmission is also needed.

In order to preserve the simplicity of the model presented here we have modeled perfectly uniform cloth, but it would be simple to add randomness to the model to achieve a more natural, irregular appearance. The size and shape of tiles as well as the parameters of the highlight could vary randomly, with correlation along threads to capture the distinctive streaks observed in fabric made with irregular thread.

References

ADABALA, N., MAGNENAT-THALMANN, N., AND FEI, G. 2003. Visualization of woven cloth. In *EGRW '03: Proceedings of the 14th Eurographics workshop on Rendering*, Eurographics Association, Aire-la-Ville, Switzerland, Switzerland, 178–185.

ASHIKMIN, M., ZE, S. P., AND SHIRLEY, P. 2000. A microfacet-based brdf generator. In *SIGGRAPH '00: Proceedings of the 27th annual conference on Computer graphics and interactive*

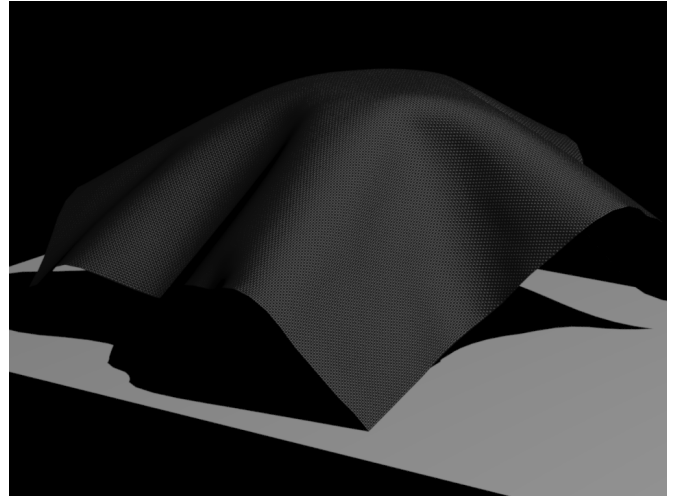


Figure 16: Rendering of a 12 cm x12 cm plain weave cloth.

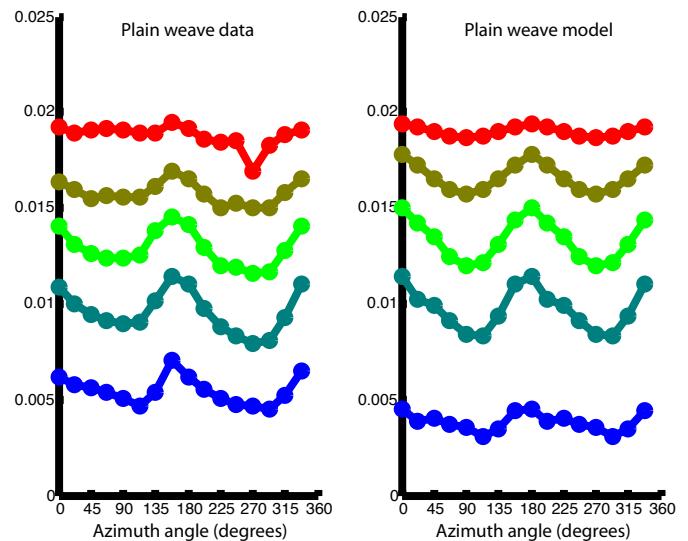


Figure 17: Plain weave BRDF comparison.

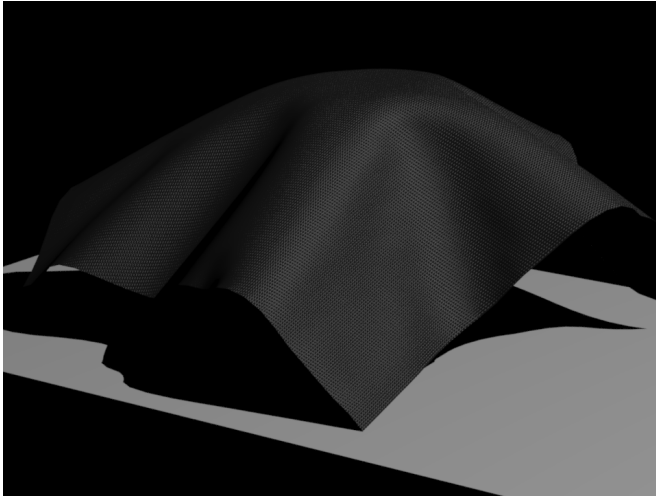


Figure 18: Rendering of a 12 cm x12 cm sateen cloth.

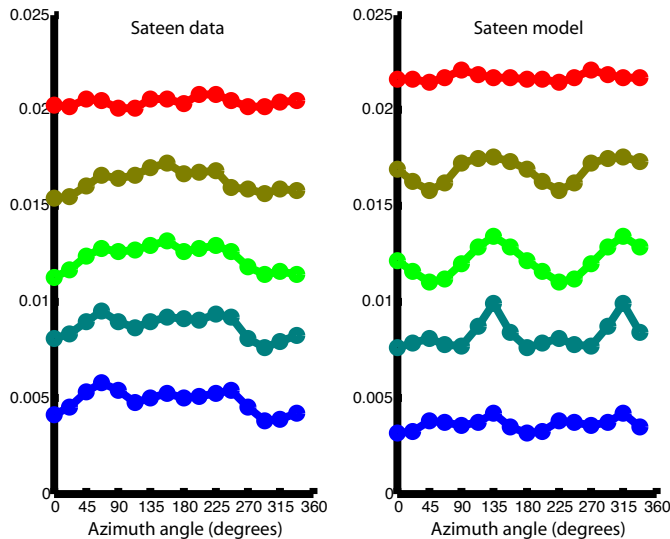


Figure 19: Sateen BRDF comparison.

techniques, ACM Press/Addison-Wesley Publishing Co., New York, NY, USA, 65–74.

DANA, K. J., VAN GINNEKEN, B., NAYAR, S. K., AND KOENDERINK, J. J. 1999. Reflectance and texture of real-world surfaces. *ACM Trans. Graph.* 18, 1, 1–34.

DRAGO, F., AND CHIBA, N. 2004. Painting canvas synthesis. *Vis. Comput.* 20, 5, 314–328.

LU, R., KOENDERINK, J. J., AND KAPPERS, A. M. L. 1998. Optical properties (bidirectional reflection distribution functions) of velvet. *Applied Optics* 37, 25, 5974–5984.

MCALLISTER, D. K., LASTRA, A., AND HEIDRICH, W. 2002. Efficient rendering of spatial bi-directional reflectance distribution functions. In *HWWS '02: Proceedings of the ACM SIGGRAPH/EUROGRAPHICS conference on Graphics hardware*, Eurographics Association, Aire-la-Ville, Switzerland, Switzerland, 79–88.

NGAN, A., DURAND, F., AND MATUSIK, W. 2005. Experimental analysis of brdf models. In *Proceedings of the Eurographics Symposium on Rendering*, Eurographics Association, 117–226.

PARKER, J. 1993. *All about cotton: a fabric dictionary & swatch-book / written and illustrated by Julie Parker*. Rain City Pub.

SATTLER, M., SARLETTE, R., AND KLEIN, R. 2003. Efficient and realistic visualization of cloth. In *EGRW '03: Proceedings of the 14th Eurographics workshop on Rendering*, Eurographics Association, Aire-la-Ville, Switzerland, Switzerland, 167–177.

USDA, A. R. S., 2005. http://www.ars.usda.gov/main/site_main.htm?modecode=35-21-00, December.

USDA, E. R. S., 2005. <http://www.ers.usda.gov/briefing/cotton/>, December.

VOLEVICH, V. L., KOPYLOV, E. A., KHODULEV, A. B., AND KARPENKO, O. A. 1997. An approach to cloth synthesis and visualization. In *The Seventh International Conference on Computer Graphics and Scientific Visualization Graphicon-97*.

WELFORD, T. 1967. *The textiles student's manual: an outline of all textile processes, from the origin of the fibre to the finished cloth; a handbook to all branches of the textiles industries*, by T. Welford. Pitman, London.

WESTIN, S. H., ARVO, J. R., AND TORRANCE, K. E. 1992. Predicting reflectance functions from complex surfaces. In *SIGGRAPH '92: Proceedings of the 19th annual conference on Computer graphics and interactive techniques*, ACM Press, New York, NY, USA, 255–264.

XU, Y.-Q., CHEN, Y., LIN, S., ZHONG, H., WU, E., GUO, B., AND SHUM, H.-Y. 2001. Photorealistic rendering of knitwear using the lumislice. In *SIGGRAPH '01: Proceedings of the 28th annual conference on Computer graphics and interactive techniques*, ACM Press, New York, NY, USA, 391–398.